

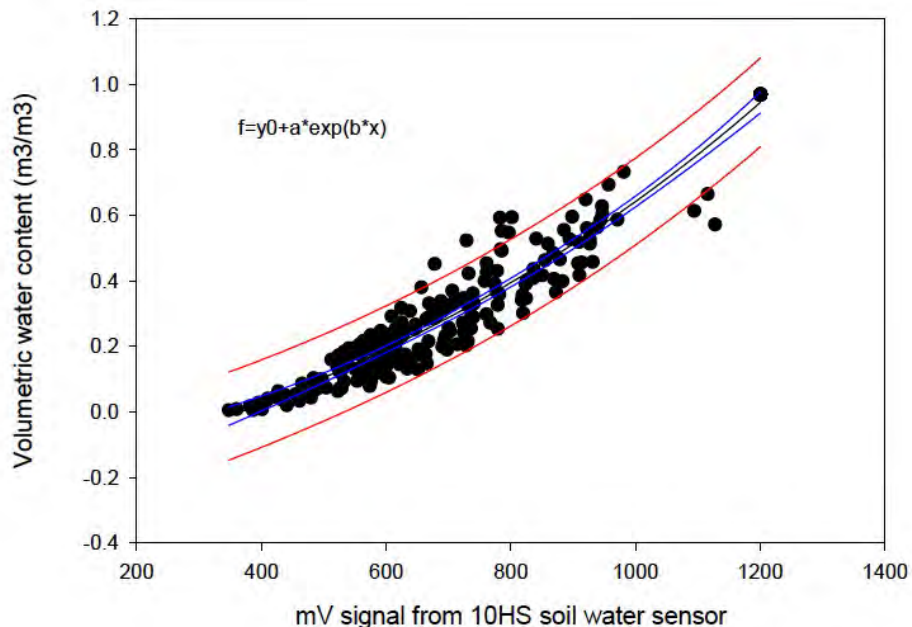
1174 Supplemental Materials for
1175

1176 **Attaining Whole-Ecosystem Warming Using Air and Deep Soil** 1177 **Heating Methods with an Elevated CO₂ Atmosphere**

1178
1179 Paul J. Hanson, Jeffery S. Riggs, W. Robert Nettles, Jana R. Phillips, Misha B. Krassovski,
1180 Leslie A. Hook, Andrew D. Richardson, Donald M. Aubrecht,
1181 Jeffrey Warren and Charlotte Barbier
1182

1183 **Surface Peat Moisture Measurements (Jeff Warren)**

1184 Intact *Sphagnum* peat monoliths were extracted from the S1-Bog into plastic containers (~7 L),
1185 and 10 replicates were taken to the Oak Ridge National Laboratory (ORNL) for calibration, and
1186 four replicates were sent to Decagon for factory calibration. One or two 10HS sensors were
1187 installed into each monolith, then water was added to the container to fully saturate the peat
1188 monolith and containers were placed into a plant growth chamber. Gravimetric water content
1189 was measured periodically as the monoliths dried down over several months and paired with the
1190 sensor mV output to create a custom calibration curve. During this period the *Sphagnum* surface
1191 (capitulum) water content was periodically assessed to derive a relationship between soil water
1192 content and surface water content – thereby providing data that is directly related to sphagnum
1193 photosynthetic activity. The ORNL- and Decagon-based soil water calibration curves were
1194 similar, and using all 14 replicates resulted in a decent curve, where volumetric water content as
1195 $VMC = -0.731 + 0.508e^{(0.00995mV)}$ where mV is the voltage signal output from the sensors
1196 ($R^2=0.92$; Supplemental Fig. S1).
1197



1198
1199 **Figure S1:** Calibration curve for the 10HS soil water sensor in peat.

1200 **Spectral Characteristics of the SPRUCE Enclosure Glazing (D. M. Aubrecht)**

1201 The spectral characteristics of the SPRUCE enclosure greenhouse panel glazing was evaluated
1202 from 250 nm to 20 microns using two radiometrically-calibrated directional hemispherical
1203 reflectance (DHR) spectrophotometers. One instrument measures UV/VNIR/SWIR (250 nm -
1204 2.5 micron) and the second measures mid- and long-wave infrared radiation (MWIR/LWIR; 2 -
1205 20 micron). All data include specular reflections.

1206
1207 The UV/VNIR/SWIR instrument is a Perkin-Elmer Lambda 750S spectrometer with a 100mm
1208 Spectralon integrating sphere and dual PMT and InGaAs detectors. The sample beam is incident
1209 at 8° from the sample surface normal. Data are collect at 1 nm resolution with 1 nm step size,
1210 and reflectance values are referenced to 99%R Spectralon. Data shown below are the mean of
1211 five independently sampled spectra.

1212
1213 The second instrument is a Thermo Scientific Nicolet iS10 FTIR spectrometer with a 3” Pike
1214 IntegratIR roughened gold integrating sphere and liquid nitrogen-cooled MCT detector. The
1215 sample beam strikes the sample surface at 12° from the surface normal. The sphere and internal
1216 beam path are purged with ultra pure dry nitrogen for 1 hour ahead of data collection in order to
1217 minimize absorption signals from CO₂ and H₂O in the atmosphere. Individual spectra are the
1218 mean of 64 samples are referenced to roughened gold. Data are presented at 4 cm⁻¹ resolution
1219 and plots below are the mean of 10 independently sampled individual spectra.

1220 Figure S2, below plots the greenhouse panel reflectance in comparison to the incoming solar
1221 spectrum (NREL “Global Tilt” data which accounts for all the solar energy that will interact with
1222 the SPRUCE enclosures), and the ideal blackbody radiation spectrum emitted by objects at 30°C
1223 and 0°C. There are two panel curves in the 2 – 2.5 micron region, where the two
1224 spectrophotomers overlap. Though the instruments give slightly different values, the overall
1225 magnitudes are in good agreement. Transmission data was also collected for the UV/VNIR, but
1226 is not shown. Transmission data for the MWIR was not collected, since at those wavelengths, the
1227 panels absorb all energy that they do not reflect.

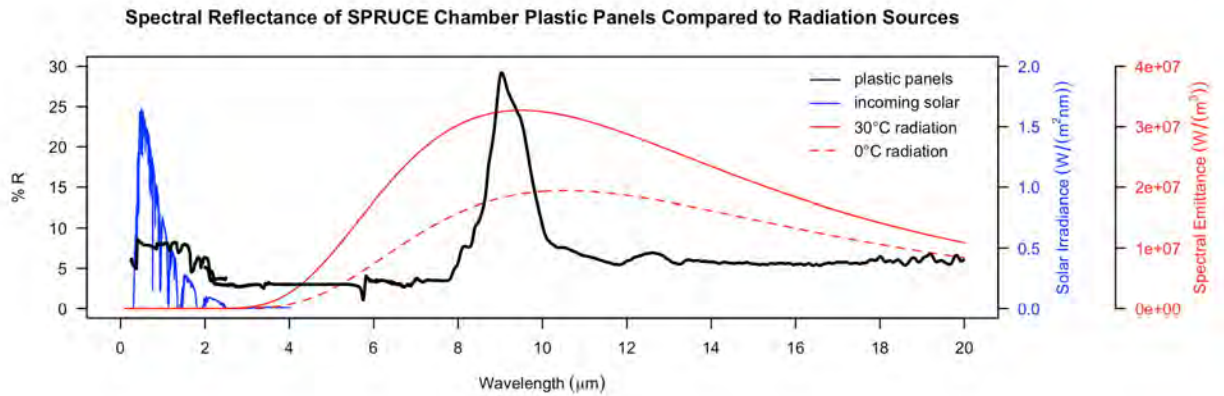
1228
1229 We note the following characteristics of the greenhouse panels:

- 1230 1) the panels absorb most of the UV and prevent it from entering the SPRUCE enclosures
1231 2) the panels transmit the majority of VNIR radiation and reflect only a small portion at these
1232 wavelengths.
1233 3) the panels absorb >90% of the incoming MWIR/LWIR radiation (>3 microns)
1234 4) the one part of the MWIR spectrum the panels reflect coincides with the peak of thermal
1235 radiation from objects that are 0-30°C (8-10 microns).

1236
1237 As the SPRUCE greenhouse panels transmit most of the VNIR wavelengths, PAR is reduced
1238 inside the enclosure, but only minimally. In the MWIR/LWIR, the story becomes more
1239 complicated. Since and the enclosure walls absorb most of the incoming radiation, the panels are
1240 likely a couple of degrees warmer than ambient air temperature when the sun is shining. In
1241 addition, the panels have a strong reflection feature at ~9 microns that reflects a fraction of the
1242 thermal energy emitted by the air, vegetation, and enclosure walls is back into the enclosure.
1243 Thermal energy from the interior that is not reflected ends up being absorbed by the panels and
1244 reemitted back into the chamber.

1245

1246 Therefore, the presence of the SPRUCE enclosure walls do not have a drastic effect on ambient
 1247 PAR for the enclosed vegetation (20% reduction, as shown in Fig. 8), with the exception of
 1248 shadows cast by the structure. However, the enclosure will minimize heat loss to the
 1249 surroundings, and keep surface conditions within the enclosures warmer day and night than
 1250 similar surfaces in the bog that are fully open to the sky. Since the frustum opening restricts
 1251 radiation losses to the sky (in terms of solid angle), the interior of the enclosure cool slower than
 1252 unchambered ambient plots, and the interior microenvironment of the enclosure behaves more
 1253 like the understory of a closed forest canopy. Instead of seeing 180° of cold, clear sky, as the
 1254 unchambered ambient plots do, the interior of SPRUCE enclosures experience a warmer
 1255 apparent sky temperature with increased incoming longwave radiation, as shown in Fig. 9.
 1256



1257 **Figure S2:** Spectral reflectance of SPRUCE enclosure plastic panels compared to radiation
 1258 sources.
 1259

1260
 1261
 1262

1263 **Air warming PID details**
1264
1265 MAU_Control = TA_2M_AVG_5minAmb + (Temp_target + Bias_Air)
1266 AirTemp_Diff = TA_2M_AVG_5min - TA_2M_AVG_5minAmb
1267 PID_Diff_Air = MAU_Control - TA_2M_AVG_5min
1268 I_Air = I_Air + P_Air
1269 If I > MaxI_Air Then I = MaxI_Air
1270 If I < -MaxI_Air Then I = -MaxI_Air
1271 P_Air_Output = P_Air * PFact_Air
1272 I_Air_Output = I_Air * IFact_Air
1273 PID_Scale = The range of temperature to scale the 4 to 20 mA control signal for the LP gas
1274 furnaces.
1275 Bias_Air = offset
1276
1277 Code from the Campbell Logger
1278
1279 P_Air = PID_Diff_Air
1280 I_Air = I_Air + P_Air
1281 If I_Air = NAN Then I_Air = 0
1282 If I_Air > MaxI_Air Then I_Air = MaxI_Air
1283 If I_Air < -MaxI_Air Then I_Air = -MaxI_Air
1284 P_Air_Output = P_Air * PFact_Air
1285 I_Air_Output = I_Air * IFact_Air
1286 PID_Air_Output = ((P_Air_Output + I_Air_Output) * PID_Scale_Air) - 3000
1287
1288 The 4 to 20 mA interface is scaled as -3000 = 4 mA and 5000 = 20 mA
1289 5000 + 3000 = 8000
1290 20 - 4 = 16
1291 16 / 8000 = .002
1292
1293 Example ((5000 + 3000) * 0.002) + 4 = 20
1294
1295 PID_Scale Example (1)
1296 If we want the range of control to be 0.6 degrees C Then 8000 / 0.6 = 13333.333
1297
1298 PID_Scale Example (2)
1299 If we want the range of control to be 3.0 degrees C Then 8000 / 3 = 2666.6666
1300
1301 Table S1. Air Temperature PID Control Settings

Treatment	Plot #	P_Fact_Air	I_Fact_Air	PID_Scale_Air	MaxI_AIR	Bias_Air
+2.25	Plot_11	0.25	0.015	8000	20	0.02
+2.25	Plot_20	0.25	0.015	8000	20	0
+4.5	Plot_4	0.3	0.08	3555.5555	20	0
+4.5	Plot_13	0.3	0.1	3555.5555	20	0
+6.75	Plot_8	0.3	0.03	2666.6666	20	0

+6.75	Plot_16	0.3	0.04	2666.6666	20	0
+9	Plot_10	0.25	0.025	2666.4000	30	0.5
+9	Plot_17	0.25	0.025	26666.4000	30	0

1302
1303
1304
1305
1306
1307
1308

Control settings for air temperature control as seen in Table S1. Air Temperature PID Control Settings are very similar but not always the same for the same treatments. This may be explained by slight differences in wind patterns across the S1 bog, differences in the efficiencies of the LP gas furnaces, and vegetation differences inside the individual plots.

1309 **Soil warming PID details**
1310
1311 PV = Process Variable (TS_200cm) A,B or C Probes
1312 $P = (TS_{200cm_Amb_Avg} + Temp\ Treatment) - PV$
1313 $I = I + P$
1314 If $I > MaxI$ Then $I = MaxI$
1315 If $I < -MaxI$ Then $I = -MaxI$
1316 $P_Output = P * Pfact$
1317 $I_Output = I * Ifact$
1318 PID_Scale = The range of temperature to scale the 4 to 20 mA control signal for the SCR's
1319 Bias_A(B,C) = offset
1320
1321 Code from Logger Program
1322
1323 $RingA = TS_{200cm_Amb_Avg} + (Temp_target + Bias_A)$
1324 $PID_Diff_A = RingA - A_{200cm}$
1325 $P_A = PID_Diff_A$
1326 $I_A = I_A + P_A$
1327 If $I_A > MaxI$ Then $I_A = MaxI$
1328 If $I_A < -MaxI$ Then $I_A = -MaxI$
1329 $P_A_Output = P_A * PFact_A$
1330 $I_A_Output = I_A * IFact_A$
1331 $PID_A_Output = ((P_A_Output + I_A_Output) * PID_Scale_A) - 3000$
1332
1333 The 4 to 20 mA interface is scaled as $-3000 = 4\ mA$ and $5000 = 20\ mA$
1334 $5000 + 3000 = 8000$
1335 $20 - 4 = 16$
1336 $16 / 8000 = .002$
1337
1338 Example $((5000 + 3000) * 0.002) + 4 = 20$
1339
1340 PID_Scale Example (1)
1341 If we want the range of control to be 0.6 degrees C Then $8000 / 0.6 = 13333.333$
1342
1343 PID_Scale Example (2)
1344 If we want the range of control to be 3.0 degrees C Then $8000 / 3 = 2666.6666$
1345
1346

1347 Table S2. Soil temperature PID control settings

Treatment	Plot #	P_Fact_ A	I_Fact_ A	PID_Scale A	P_Fact_ B	I_Fact_ B	PID_Scale B	P_Fact_ C	I_Fact_ C	PID_Scale C	MaxI	Bias_ A	Bias_ B	Bias_ C
+2.25	PLOT_11	0.6	0.0015	4000	0.6	0.0015	4000	0.6	0.0015	4000	100	0	0	0.11
+2.25	PLOT_20	0.6	0.0015	4000	0.6	0.0015	4000	0.6	0.0015	4000	100	0	0	0
+4.5	PLOT_4	1.5	0.0011 3	3555.5555	1.6	0.0011 3	3555.5555	1.85	0.0011 3	3555.555	100	0	0.07	0.07
+4.5	PLOT_13	1.65	0.0011 3	3555.5555	1.6	0.0011 3	3555.5555	1.85	0.0011 3	3555.5555	100	0.15	0	0.1
+6.75	PLOT_8	2.1	0.0085	2666.6666	2.1	0.0015	2666.6666	2.2	0.0015	2666.6666	100	0.12	0.15	0.3
+6.75	PLOT_16	2.1	0.0035	2666.6666	2.1	0.0085	2666.6666	2.2	0.003	2666.6666	100	0.26	0.2	0.15
+9	PLOT_10	2.1	0.0015	2666.6666	2.1	0.0015	2666.6666	1.7	0.0015	2666.6666	100	0.4	0.43	0.2
+9	PLOT_17	2.1	0.0015	2666.667	2.1	0.0015	2666.667	1.7	0.0015	2666.667	100	0.45	0.13	0.34

1348
1349
1350
1351

1352 Table S3. Time required to reach DPH differentials by treatment plot.

Plot	Treatment (°C)	Date Soil Temp Monitoring Began	Date Treatment Began	Time Treatment Began (CST)	Days to Achieve Target °C Differentials for A and B Series within each plot
6	Control (+0)	2/25/14	NA	NA	0
19	Control (+0)	6/18/14	NA	NA	0
10	+9	5/19/14	6/17/14	14:00	81
17	+9	6/9/14	6/17/14	16:00	66
8	+6.75	5/20/14	6/25/14	9:30	94
16	+6.75	6/9/14	6/23/14	15:55	71
4	+4.5	2/25/14	7/2/14	13:00	58
13	+4.5	5/20/14	6/26/14	13:30	51
11	+2.25	5/20/14	7/1/14	13:00	22
20	+2.25	6/17/14	6/25/14	10:00	24

1353
1354
1355

1356

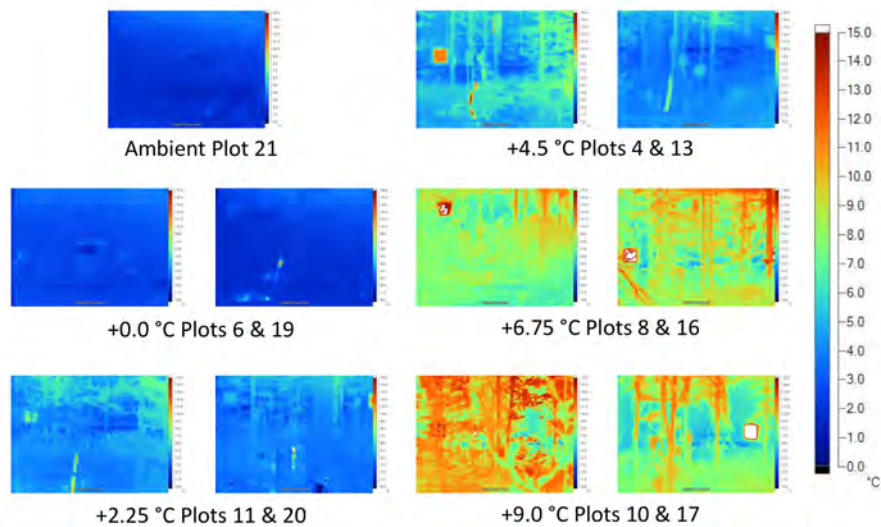


1357
1358
1359
1360
1361
1362
1363

Figure S3: Left photograph is a completed SPRUCE warming enclosure, and the right photograph shows the subtending hydrologic corral that lies beneath each enclosure. The encircling and interlocked sheet piles extend through the peat to the ancient lake bed below, and effectively isolate the hydrology of the enclosure.

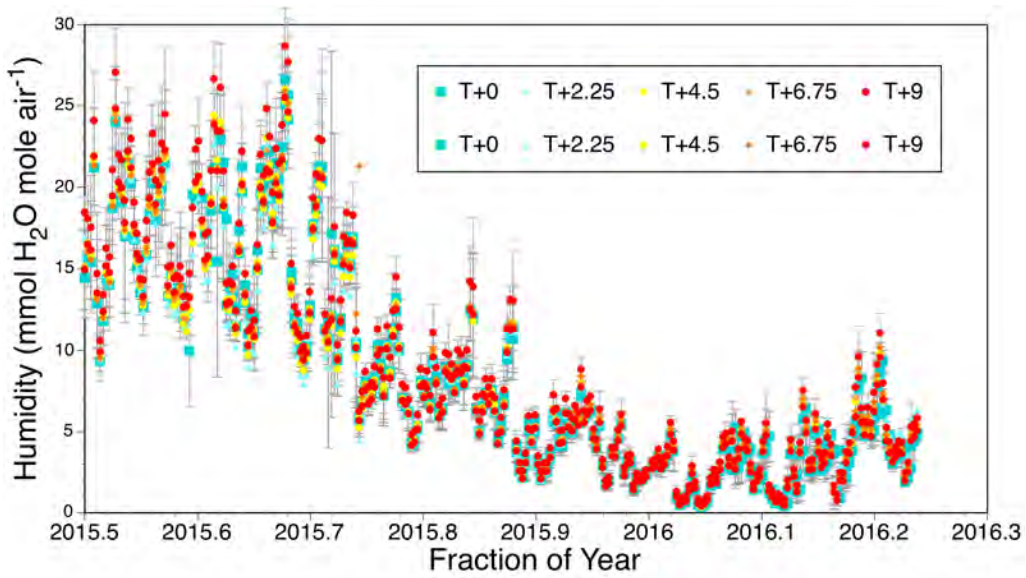
Whole Ecosystem Warming In Pictures

(6 November 2015; IR thermal Images)



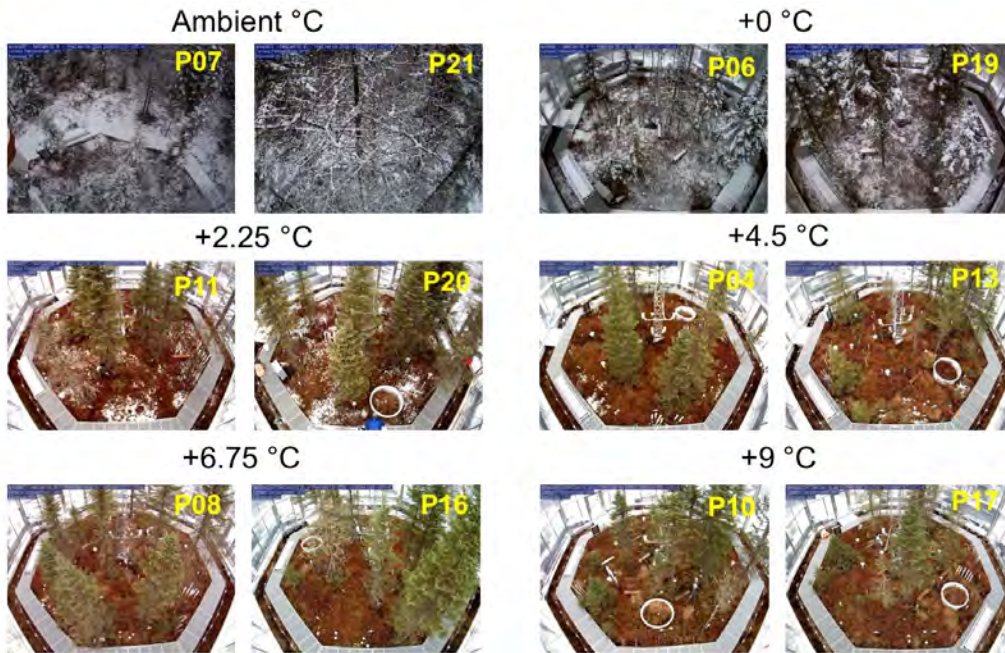
1364
1365
1366
1367
1368
1369

Figure S4: Color infrared images for the space within the designated treatment enclosures and an unchambered ambient plot recorded on November 6, 2015 just before sunrise within a 30-minute period. The thermal color scale in °C applies to all images. Non-biological metal or plastic surfaces in the images may not provide an accurate temperature due to their emissivity difference from biological surfaces.



1370
1371
1372
1373
1374
1375

Figure S5: Absolute humidity by treatment enclosure from mid-year 2015 through early 2016. For clarity of the image, standard error bars all in grey are included only for the control (T+0) and the warmest (T+9) plots.

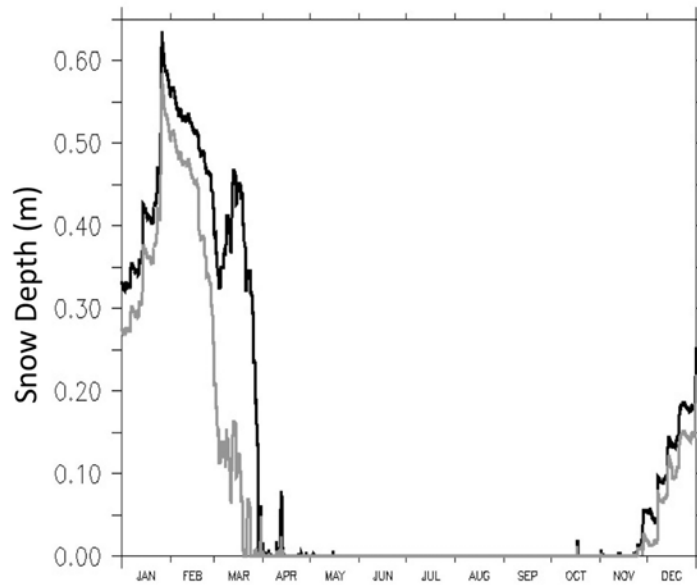


1376
1377
1378
1379
1380
1381
1382

Figure S6: Images of snow accumulation at unchambered ambient locations and within all treatment enclosures by target warming temperature differentials at 10:00 on 6 April 2016. Little obvious snow accumulation is apparent above the +4.5 °C treatment, even though precipitation in the form of snow does enter all enclosures.

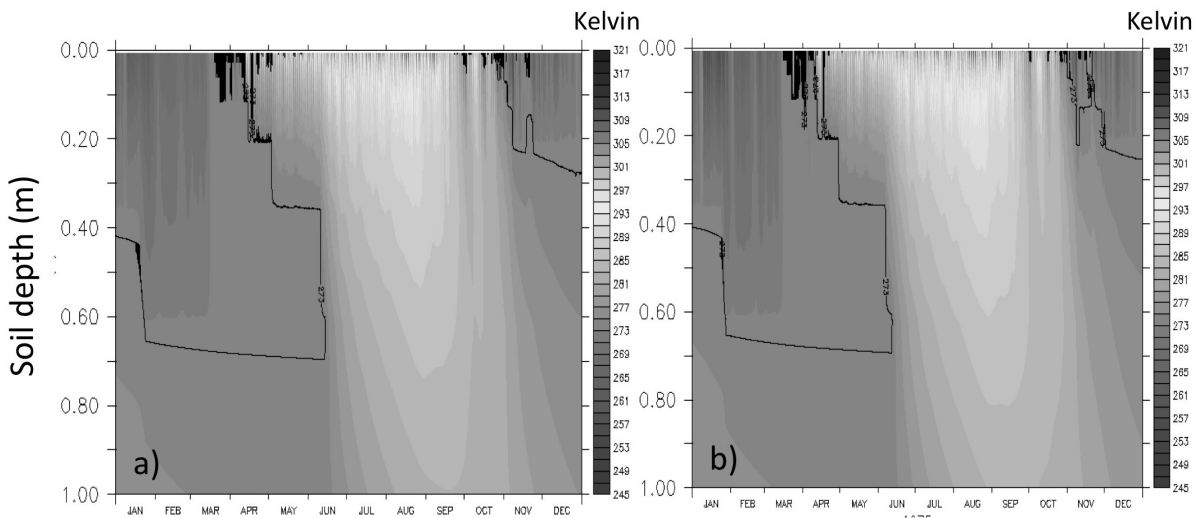
1383
1384
1385

Additional graphics from the SPRUCE Enclosure Energy Simulations (D. Ricciuto)



1386
1387
1388
1389
1390

Figure S7: Simulations of snow depth for ambient conditions (black) and within an enclosure (grey) using driver meteorology data from 2013.



1391
1392
1393
1394
1395
1396

Figure S8: Profiles of simulated top 1m soil temperature in ambient (a) and enclosure (b) simulations. Contour colors represent peat temperatures in degrees kelvin, and the black contour indicates those layers that are below freezing during the year. Ice depths are similar between the simulations.

1397 **Elevated CO₂ Protocol Details**

1398
 1399 During the period from January through March 2016 when biological activities were minimal,
 1400 various test were conducted on Plot 19 (a constructed control), Plot 11 (+2.25 °C), Plot 4 (+4.5
 1401 °C), Plot 8 (+6.75 °C) and Plot 10 (+9 °C) to establish the CO₂ addition control protocols. Over a
 1402 multi-day period with variable winds, a fixed amount of CO₂ ranging from 150 to 300 l min⁻¹ of
 1403 pure CO₂, depending on target temperature levels, was added to the enclosure for a multiple day
 1404 period to generate a profile of achieved CO₂ differentials (mean at 0.5, 1 and 2 m heights) as a
 1405 function of the wind velocities measured at +10 m. A fitted relationship between wind velocity at
 1406 +10 m and enclosure fractional air turnover volumes (assuming and enclosure volume of 911 m³)
 1407 was derived from these data. Instantaneous measured wind velocities were then applied to a
 1408 turnover fraction equation to estimate the amount of CO₂ to be added to achieve a +500 μmol
 1409 mol⁻¹ value over ambient-CO₂ measured within the constructed control plot (i.e., Plot 6). An
 1410 example is as follows:

1411 $TF = (0.00001330297 * WS^6) + (-0.0003804215 * WS^5) + (0.003932579 * WS^4) +$
 1412 $(-0.01517648 * WS^3) + (-0.004974471 * WS^2) + (0.2532064 * WS)$

1413 where TF is enclosure turnover fraction (unit less), and WS is wind velocity (m s⁻¹). The form of
 1414 the TF equation might also be a simple exponential function depending on the calibration data
 1415 set for a given plot.

1416
 1417 Using the TF value, an initial coarse control value for CO₂ addition was calculated as:

1418 $Course\ CO_2\ Addition = CCO_2 = EV * TF * DeltaCO_2 * 1000$

1419 where CCO₂ is the CO₂ addition rate in l min⁻¹, EV is the enclosure volume in m³ (~910 m³),
 1420 DeltaCO₂ is the desired target increase in CO₂ above ambient conditions (500 μmol mol⁻¹ or
 1421 0.0005 m³ m⁻³), and 1000 allows for the conversion from m³ to liters. To further account for the
 1422 variation in enclosure turnover times with external winds the DeltaCO₂ values were
 1423 supplemented with added amounts as shown in the following table.

1424
 1425 Table S4. DeltaCO₂ adjustment values for low, medium and high winds by treatment plot. C

CO ₂ Treatment Plot #	Low Wind Adjustment (ppm)	Medium Wind Adjustment (ppm)	High Wind Adjustment (ppm)
4	50	50	50
10	125	75	40
11	75	75	75
16	50	25	0
19	75	50	0

1426
 1427 Yet additional fine control to achieve target differential CO₂ concentrations within the enclosure
 1428 was based on a feedback adjustment defined by the error in achieving +500 μmol mol⁻¹.

1429 $CO_2ERR = 500 - (CO_2Enclosure - CO_2Ambient)$

1430
 1431 $Final\ CO_2\ Addition = FCO_2 = (910.6 * CO_2ERR)/1000000*1000*1.15$

1432 where CO₂ERR is the observed difference of enclosure CO₂ when compared with CO₂ in the
 1433 constructed control (Plot 6), 1000000 and 1000 convert m³ to L, and 1.15 is an arbitrary valued
 1434 needed to achieve good results (probably accounting for unmeasured vertical winds). This

1435 combined control algorithm reevaluated every 10 seconds during active CO₂ additions, allowed
 1436 us to achieve target CO₂ levels within the enclosure within a $\pm 50 \mu\text{mol mol}^{-1}$ band around our
 1437 target of + 500 $\mu\text{mol mol}^{-1}$ CO₂. We will continue to adjust the algorithm for CO₂ additions as
 1438 we operate to allow each enclosure to achieve $+500 \pm 25 \mu\text{mol mol}^{-1}$ for all wind conditions and
 1439 temperature treatments.

1440
 1441 Elevated CO₂ additions are only made during daytime hours as a cost reducing measure, because
 1442 past studies have shown that there is no direct effect of elevated CO₂ on respiratory processes
 1443 (Amthor 2000, Amthor et al. 2001, Toiler et al. 2001). The elevated CO₂ treatments are initiated
 1444 or stopped each day based on calculated solar angles for each day of the year using the Solpos
 1445 algorithm developed by the National Renewable Energy Laboratory (NREL).

1446
 1447 Table S5. Mean daily differential CO₂ achieved from 19 August to 1 September 2016. NA = not
 1448 applicable.

Warming Level and Plot	Differential [CO ₂] in ppm \pm sd
Reference Plot - +0.00 °C Plot 06	NA
+2.25 °C Plot 20	-9 \pm 8
+4.50 °C Plot 13	-0.1 \pm 8
+6.75 °C Plot 13	-13 \pm 9
+9.00 °C Plot 04	1 \pm 11
eCO ₂ +0.00 °C Plot 19	483 \pm 22
eCO ₂ +2.25 °C Plot 11	471 \pm 21
eCO ₂ +4.50 °C Plot 04	490 \pm 13
eCO ₂ +2.25 °C Plot 16	511 \pm 15
eCO ₂ +9.00 °C Plot 10	480 \pm 73

1449

1450

1451 Supplemental Literature

1452 Amthor, J.S.: Direct effect of elevated CO₂ on nocturnal in situ leaf respiration in nine temperate
 1453 deciduous tree species is small. *Tree Physiol.* 20, 139-144, 2000.

1454

1455 Amthor, J.S., Koch, G.W., Willms, J.R., Layzell, D.B.: Leaf O₂ uptake in the dark is independent
 1456 of coincident CO₂ partial pressure. *J Exper Bot*, 52, 2235–2238, 2011.

1457

1458 Tjoelker, M.G., Oleksyn, J., Lee, T.D., Reich, P.B.: Direct inhibition of leaf dark respiration by
 1459 elevated CO₂ is minor in 12 grassland species. *New Phytol*, 150, 419–424. doi:10.1046/j.1469-
 1460 8137.2001.00117.x, 2001.